Pulsed Plasma Deposition from 1,1,2,2-Tetrafluoroethane by Electron Cyclotron Resonance and Conventional Plasma Enhanced Chemical Vapor Deposition

CATHERINE B. LABELLE, KAREN K. GLEASON

Department of Chemical Engineering, Massachusetts Institute of Technology, Cambridge, Massachusetts 02139

Received 8 September 1999; accepted 28 March 2000

ABSTRACT: Pulsed electron cyclotron resonance (ECR) plasmas from 1,1,2,2-$C_2H_2F_4$ are used to deposit fluorocarbon films. The deposited films have a F : C ratio of 1, with only slight variations in % CF_x as the deposition pressure is decreased. The optical emission (OES) spectra of the pulsed $C_2H_2F_4$ plasmas show high intensity peaks for H, C_2, and C_3, with lower intensity CF_2 and F peaks. The dominant OES peak shifts from H_α to C_2 when the pressure is reduced, most likely a result of the increased electron temperature at the lower pressure. Gas-phase recombination reactions may be occurring between the OES sampling region and the deposition substrate (~ 8-in. distance), producing fluorocarbon molecular deposition species, thus accounting for the high degree of fluorination in the deposited films. Parallel plate plasma deposited films from $C_2H_2F_4$ show less fluorination than their ECR counterparts, as well as vastly different OES spectra, with CF_2 peaks dominating the spectra versus H and C_2. The presence of ion bombardment in the parallel plate system tends to defluorinate the depositing films, and thus can account for the less fluorinated films deposited in the parallel plate versus ECR systems. © 2001 John Wiley & Sons, Inc. J Appl Polym Sci 80: 2084–2092, 2001

Key words: electron cyclotron resonance; optical emission spectroscopy; plasma deposition; fluorocarbon; $C_2H_2F_4$

INTRODUCTION

Fluorocarbon plasmas are used extensively throughout the semiconductor industry in both etching and cleaning processes.[1,2] The plasma deposition of fluorocarbon films has been studied for many years,[3,4] but it has only recently been considered for use in low κ applications.[5] These low κ materials would yield reductions in propagation delay, power consumption, and cross-coupling noise between adjacent lines, all of which would enable the implementation of future generations of integrated circuit design rules.[6–9] In order to implement these new materials, however, a host of film property and processing requirements, some of which conflict, must be met.[6–8] Therefore, the ability to tailor a process to produce films with a specific set of properties is desirable.

A variety of different precursors are currently used in plasma enhanced chemical vapor deposition (PECVD), including CF_4, C_2F_4, C_2F_6, C_3F_8, c-C_4F_8, C_6F_6, CHF_3, CH_2F_2, $C_2H_2F_4$, and C_3F_6O (hexafluoropropylene oxide, HFPO).[3,10–12] Surprisingly, however, it has been found that films of similar composition can be deposited from dissim-

Correspondence to: K. K. Gleason.

Contract grant sponsors: Lucent Technologies Bell Laboratories Graduate Research Program for Women; Tokyo Electron Limited.

Contract grant sponsor: National Science Foundation; contract grant number: DMR-9400334.

Journal of Applied Polymer Science, Vol. 80, 2084–2092 (2001)

ilar precursors. For example, films having F : C ratios between 1.0 and 1.3 have been grown from CF_4, C_2F_6, C_4F_8, C_9F_{18}, and CHF_3 using both conventional parallel plate and high density plasma sources.[10,13–16] In an effort to expand the range of film compositions, gas mixtures have been investigated. Typical additives include H_2 and O_2,[17,18] while mixtures of hydrofluorocarbons with pure fluorocarbons (e.g., $C_4F_8 + CH_4$)[19,20] or linear fluorocarbons with cyclic fluorocarbons (e.g., $C_2F_6 + C_6F_6$) are also being studied.[21,22]

More recently, the use of pulsed plasmas as a means to control the plasma deposition environment has gained recognition.[11,16,23,24] In this process, radiofrequency power is applied for a specified "on" time, followed by an "off" period during which no excitation is used. During the on time both ions and reactive neutrals are produced. However, because ions often have shorter lifetimes than neutrals, during the off time the ratio of neutrals to ions will increase; thus, the process equilibrium will be shifted to favor film deposition from reactive neutrals. Therefore, the overall chemistry of these plasmas should be much more sensitive to the original precursor molecules than their continuous counterparts, and it should be possible to develop a range of fluorocarbon films with different film properties from a single precursor.

Several pulsed plasma chemistries employing capacitively coupled plasma sources (i.e., parallel plate reactors) have been studied in detail.[11,16,23,25,26] Typically, pulse modulation on the millisecond scale is used for these low density plasmas. For HFPO,

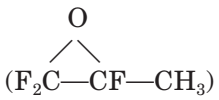

the film composition changes dramatically with pulse off time. At very short pulse off times (10 ms on, 20–60 ms off) the films contain almost equal fractions of CF_3, CF_2, CF, and quaternary carbon (C—CF), whereas at longer pulse off times the film composition becomes increasingly dominated by CF_2.[11,23,27,28] Similar control for CF_3 has been observed for pulsed plasma deposition from a trimer of C_9F_{18} compounds.[16] Deposition from other feed gases such as 1,1,2,2-$C_2H_2F_4$ and CH_2F_2 is less influenced by the pulse on and off times, in this case, mainly due to competing dissociation pathways.[25,26]

The use of pulsed power modulation in high density plasma (HDP) systems has been less widely investigated. Two different pulse timing regimes are employed for HDP processes. Typically, microsecond pulsing is used in etching applications where it has been found to be very effective at reducing notching effects, both in electron cyclotron resonance (ECR)[29–31] and inductively coupled plasmas (ICPs).[32] Periods of 10–100 μs are used for both on and off pulse times. For deposition, some researchers use microsecond pulsing, usually with ICP sources,[33,34] while others use millisecond pulsing, usually with ECR sources.[14,35] Pulse times for the deposition processes range from 10–400 μs and 10–20 ms for on times, and 5–400 μs and 10–100 ms for off times. Takahashi et al.[14,17,18,35–37] have closely examined the gas-phase characteristics of millisecond-pulsed ECR plasmas from CHF_3, as well as the resulting films. As in the parallel plate pulsed plasma systems, films deposited in the ECR system also displayed a variation in composition due to both the pulse conditions and the addition of either H_2 or O_2 to the feed gas.[17,18] However, it should be noted that CHF_3 is the only (hydro)fluorocarbon precursor which has been studied in detail in a millisecond-pulsed ECR plasma.

In this work, millisecond-pulsed ECR plasmas from 1,1,2,2-$C_2H_2F_4$ have been used to deposit fluorocarbon films. The composition of each film was determined by carbon 1s X-ray photoelectron spectroscopy (C1s XPS), while optical emission spectroscopy (OES) was employed during deposition to identify the primary optically excited species present in the pulsed plasmas. The ECR film compositions are distinctly different from the corresponding films deposited in a conventional parallel plate reactor. The differences in deposition environments between the parallel plate reactor and the ECR reactor were clearly evident in the OES spectra from each reactor.

EXPERIMENTAL

Figure 1 shows a schematic of the HDP system, which is equipped with a Wavemat MPDR 325i ECR source employing cavity tuning. The plasma is generated in a quartz bell jar and confined by a set of permanent magnets that extend 5 in. below the bell jar. The gas inlet is located directly under the quartz bell jar. Five-inch diameter silicon (Si) wafers are placed in the mechanically clamping wafer chuck via a load lock equipped with a trans-

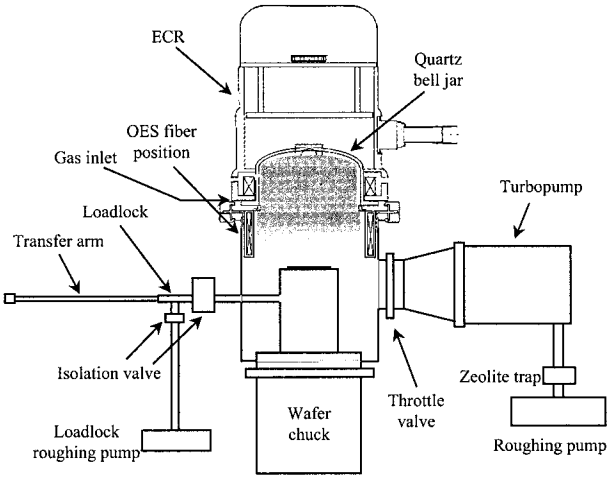

Figure 1 A schematic of the electron cyclotron resonance (ECR) deposition system. It is equipped with a Wavemat MPDR 325i ECR source employing cavity tuning, a 5-in. diameter mechanically clamping wafer chuck, and a load lock entry system. The pulsed microwave excitation is provided by a Muegge Electronics Model ML1250D-100TE low ripple, pulsable power supply operating at 2.45 GHz and 1.25 kW and capable of pulsing up to 25 kHz. Millisecond pulsing was employed in these experiments.

fer arm. The deposition surface is ~ 5 in. below the magnetic confinement ring. The wafer chuck is equipped for independent biasing and He backside cooling; however, neither bias nor cooling was utilized in these experiments since it was found that there was insignificant wafer heating when bias was not employed. The ECR system was evacuated using a 3300 L/s turbomolecular pump (TH3000M, Osaka Vacuum) backed by a 50 ft^3/min (cfm) roughing pump (2063, Alcatel). Typical base pressures of ~ 10^{-7} Torr were achieved with the elastomer (Viton) O-ring seals used in the system. Operating pressures ranged from 2–10 mTorr.

Pulsed microwave plasma excitation was generated by a Muegge Electronics ML1250D-100TE low ripple, pulsable power supply operating at 2.45 GHz and 1.25 kW, which was capable of pulsing up to 25 kHz. The timing for the microwave power supply was driven by a variable dc voltage signal from a Systron–Donner 110 C pulse generator.

Plasmas were generated from 1,1,2,2-$C_2H_2F_4$ using a pulse on time of 10 ms and pulse off times of 50 and 100 ms. The precursor flow rate was 50 sccm, while the chamber pressure was set to 3, 5, or 10 mTorr. Peak powers of either 750 or 1000 W were used during the pulse on time.

Film thicknesses and refractive indices were determined by single-wavelength ellipsometry (Rudolph Research AutoEl II Ellipsometer, Gaertner Scientific Corporation L116A Ellipsometer). Single-wavelength ellipsometry was done with a He—Ne laser (6328 Å) at an angle of incidence of 70°. The magnitude of the film thicknesses was confirmed by profilometry (Tencor P-10 surface profilometer). *In situ* laser interferometry was used to monitor film growth during deposition.

The C1s XPS (Physical Electronics 5200C employing a Mg K$\alpha_{1,2}$ exciting radiation source) was used to determine the relative concentrations of CF_3, CF_2, CF, and C—CF in each deposited film using the same analysis method techniques as Limb et al.[23] The F : C ratios were calculated from the regressed CF_x concentrations.

Plasma species were monitored by OES. An Ocean Optics S2000 OES configured with a 10-μm slit, 200–800 nm grating, and a UV/VIS upgrade was used in conjunction with a 600-μm optical fiber equipped with a UV collimating lens. The OES was operated in scope mode, in which the raw light intensity from the plasma was sampled. A dark spectrum was subtracted from each spectrum. Spectral integration times were optimized for each plasma condition to obtain a strong signal. Typical integration times varied from 500 to 2000 ms.

Actinometry involves comparing the emission intensity of a species of interest with that of an inert species added to the feed gas.[38] Only a small amount of the inert gas is added in order to minimize its effect on the plasma as a whole. The emission intensity for species i from a particular excited state can be expressed as

$$I_i = \Gamma_i k_i [e-][i] \tag{1}$$

where I_i is the intensity of the emission from species i (either the species of interest X or the actinometer), Γ_i is the branching ratio for emission relative to all other de-excitation paths, k_i is the excitation efficiency for species i, [e−] is the electron density, and [i] is the concentration of species i.[39] The excitation efficiency, k_i, is a function of the electron energy distribution and the excitation cross section:

$$k_i = \int_0^\infty v(\varepsilon)\sigma_i(\varepsilon)f(\varepsilon)\, d\varepsilon \tag{2}$$

where ε is the electron energy, $v(\varepsilon)$ is the electron velocity, $\sigma_i(\varepsilon)$ is the collision cross section for the excitation of i, and $f(\varepsilon)$ is the electron energy distribution.[39] Actinometry allows calculation of unknown species densities by scaling the emission intensity of a particular species of interest X, with the emission intensity of the actinometer:

$$\frac{I_X}{I_{\text{act}}} = \frac{\Gamma_X k_X [\text{e}-][X]}{\Gamma_{\text{act}} k_{\text{act}} [\text{e}-][\text{act}]}. \quad (3)$$

For the emission intensities to be directly proportional to the species concentrations, $\Gamma_X k_X / \Gamma_{\text{act}} k_{\text{act}}$ must be constant. Therefore, valid actinometry requires that the actinometer and species X undergo the same excitation path (electron impact), the relaxation occurs exclusively by photoemission or by photoemission plus a parallel de-excitation pathway with a constant branching ratio, and that both species have similar cross-section functionality with energy.[38,39]

Actinometry is commonly used to measure F concentrations in fluorocarbon plasmas using an Ar actinometer, where these conditions are met.[38,40,41] However, application of actinometry to molecular species such as CF_2 is more complicated, since the molecular and actinometer threshold energies are typically significantly different. For example, the excitation threshold of CF_2^* is $\sim$ 4.5 eV, while that of Ar* is 13.5 eV (for the 750.4 nm emission line).[39] Molecular actinometers such as N_2 have been used,[42] but the system is complicated by the potential dissociation of N_2. Recent work by Kiss et al. has suggested relaxing the excitation threshold matching requirement in cases where the electron energy distributions can be assumed constant.[39] They have found for a CF_4 plasma system that this assumption is valid over a range of process conditions (500–1000 mTorr, 20–100 W) and that actinometry can be applied to the molecular species present in order to compare two different spectra.

A small percentage of Ar (2 sccm) was added to most runs discussed in this work in order to allow normalization of the spectra via actinometry. It is assumed that the electron energy distributions remain relatively constant for the parameter space investigated. Table I lists OES emission assignments used in this work.[43,44]

RESULTS AND DISCUSSION

Figure 2 shows C1s XPS spectra for films deposited at 10, 5, and 3 mTorr, all from 50 sccm of $C_2H_2F_4$ under 10 ms on/50 ms off (10/50) pulsed ECR excitation. A peak power of 750 W was used at 10 mTorr, while 1000 W was used at 5 and 3 mTorr. These peak powers correspond to average powers of $\sim$ 125 and $\sim$ 165 W, respectively. Each spectrum has been normalized to the same total integrated area. Table II lists the percentage of each CF_x (x = 1–3) species, the F : C ratio, and the refractive index for each film.

A slight shift from CF_3 to CF_2 species (Fig. 2) occurrs as the pressure is reduced from 10 to 5 mTorr, but otherwise the spectra appear to be identical. Table I shows similar F : C ratios and refractive indices for all three films. The slight compositional change may be due to the higher peak power employed at the lower pressure (1000 vs. 750 W), which would promote increased surface rearrangement. A higher peak power was used at the lower pressure since it was difficult to strike a plasma at the lower power level, but the average powers are similar enough to warrant comparison of the deposited films. Films deposited at 3 and 5 mTorr with 10/100 pulsed plasmas (not shown) had similar compositions, although a small shift to less fluorinated structures was observed in the film deposited at 5 mTorr. Longer pulse off times were attempted, but a stable plasma could not be maintained. No peaks were observed in the Fourier transform IR (FTIR) spectra (not shown) between 2700 and 3300 cm^{-1}, indicating that no hydrogen is incorporated into any of the films deposited from $C_2H_2F_4$.

Figure 3 shows OES spectra from 10/50 $C_2H_2F_4$ pulsed plasmas at 10, 5, and 3 mTorr, all using 50 sccm $C_2H_2F_4$. The spectra are dominated by C_2, C_3, and H species, with lower intensity CF_2 and F peaks. A small amount of Ar (2 sccm) was included as an actinometer and each spectrum has been normalized to the 750.3-nm Ar peak intensity. It is actually quite surprising that, given the elemental and nonfluorinated nature of the species observed by OES (H, C_2), the deposited films contained relatively large concentrations of CF_2 and CF_3. These spectra were taken at a position in the chamber approximately 8 in. above the deposition substrate. Typical mean free paths at 10 mTorr are on the order of millimeters[45]; therefore, it is possible that, rather than carbon depositing on the substrate and undergoing subsequent fluorine addition, gas-phase recombination reactions are occurring, resulting in molecular fluorocarbon deposition species. Diamond deposition from ECR plasmas of $CH_4 + H_2$ show some evidence of gas-phase recombination,

Table I Optical Emission Spectroscopy Wavelength Assignments

Species	OES Wavelength (nm)	Emission Band System
CF_2	245–321	
C_2	516.5	Swan system
	473.7	↓ Decreasing intensity
	563.6, 558.6, 471.5	
	469.8	
	512.9	
C_3	405.1	Comet-head group
CH	431.4	4300-Å System
CO	561.0, 519.8, 483.5, 451.1	Ångström system
	283.3	Third positive system
	297.7	↓ Decreasing intensity
	313.4	
	330.6	
	349.3	
H	656.2	H_α
	486.1	H_β
	434.0	H_γ
F	685.6	↓ Decreasing intensity
	703.7	
	712.8	
	775.4	
	690.2, 720.2, 731.1, 780.0	
	624.0	
	634.8, 739.9	
C	283.7, 426.7, 723.6	
Ar	811.5	↓ Decreasing intensity
	801.5, 763.5	
	810.4, 800.6, 794.8, 750.3	
	772.4	
	738.4, 706.7, 696.5	

Adapted from Reader and Corliss[43] and Pearse and Gaydon.[44]

where H, CH, and C_2 species are detected in the bulk plasma via OES, but CH_3 is acknowledged as the primary deposition species.[46–49]

The most striking feature of Figure 3 is the dramatic increase in the intensity of the C_2 peak at 516.5 nm as the pressure is reduced. At 10 mTorr the primary peak is H_α (656.2 nm), with the 516.5 nm C_2 peak is a close second. However, as the pressure is reduced, the intensity of that C_2 peak increases, strongly dominating over the H_α peak. The shift in plasma species is seen more clearly in Figure 4, which shows the intensities of F (703.7 nm), H_α (656.2 nm), C_2 (516.5 nm), C_3 (405.1 nm), CH (431.4 nm), and CF_2 (251.9 nm) as a function of pulsed plasma pressure, all are normalized to the Ar actinometer. A large increase in intensity is seen for C_2, while more moderate increases are seen for F, H_α, and CH. The C_3 peak intensity remains nearly constant, while that of CF_2 decreases slightly. The electron temperature of ECR plasmas has been seen to increase with decreasing pressure due to the decreased number of collisions that electrons undergo with neutrals.[50,51] The corresponding increase in high energy electrons could result in more efficient fracturing of the precursor molecule, producing the shift in dominant pulsed plasma species. However, despite the changing pulsed plasma species concentrations, the deposited films are nearly identical (Fig. 2). This observation further indicates that the pulsed plasma species observed via OES may not be representative of the actual species depositing on the wafer surface.

Finally, Figure 5(a,b) shows the C1s XPS and OES spectra for a 10/100 $C_2H_2F_4$ pulsed plasma film deposited in a parallel plate PECVD reactor. Conventional PECVD films deposited from $C_2H_2F_4$ have been studied in detail previously,[25,26]

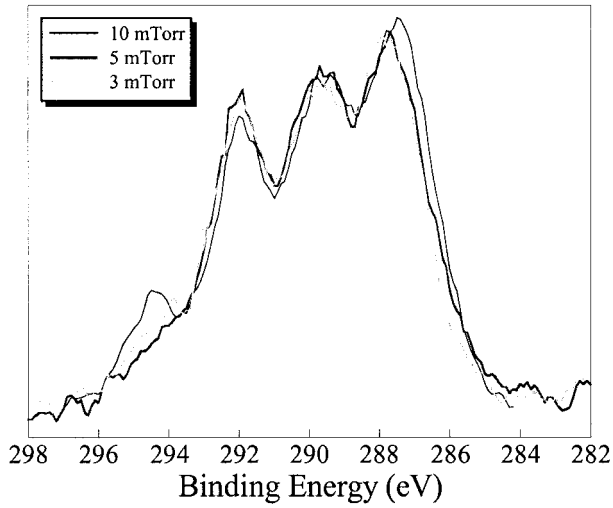

Figure 2 Carbon 1s XPS spectra for 10 ms on/50 ms off (10/50) $C_2H_2F_4$ pulsed ECR plasma films deposited at 10, 5, and 3 mTorr using 50-sccm feed gas. A peak power of 750 W was used at 10 mTorr, while 1000 W was used at 5 and 3 mTorr. Each spectrum has been normalized to the same total integrated area. A slight shift from CF_3 to CF_2 species occurs as the pressure is reduced from 10 to 5 mTorr, but otherwise the spectrum appear identical. The slight compositional change may be due to the higher peak power employed at the lower pressure (1000 vs. 750 W), which would promote increased surface rearrangement.

and a representative sample is presented here for comparison to the ECR films. The film composition does not change significantly with pulse off time for these films, and so the 10/100 film in Figure 5 is valid for comparison to the 10/50 pulsed ECR plasma films discussed above. A comparison of Figure 5(a) with Figure 2 makes it clear that the parallel plate plasma film is distinctly different from those obtained by pulsed ECR, most notably with a much higher C—CF fraction. The differences in the plasmas are even more pronounced, which a comparison of Figure 5(b) with Figure 3 shows. An Ar actinometer was not available in the parallel plate system, and therefore Figure 5(b) has not been normalized. However, it is clear that the CF_2 OES peaks are overwhelmingly dominant in the parallel plate

Table II Percentages of CF_3, CF_2, CF, and C—CF Species and F : C Ratios

Film	CF_3 (%)	CF_2 (%)	CF (%)	C—CF (%)	F : C	N_f
10 mTorr	8	23	32	37	1.01	1.47
5 mTorr	6	26	32	37	1.00	1.45
3 mTorr	7	26	29	39	1.01	1.45

The percentages were obtained from C1s XPS for films deposited using 10/50 pulsing from $C_2H_2F_4$. The $C_2H_2F_4$ flow rate was 50 sccm for all films. Peak powers of 750 and 1000 W were used for 10 mTorr and lower pressure (3 or 5 mTorr) depositions, respectively.

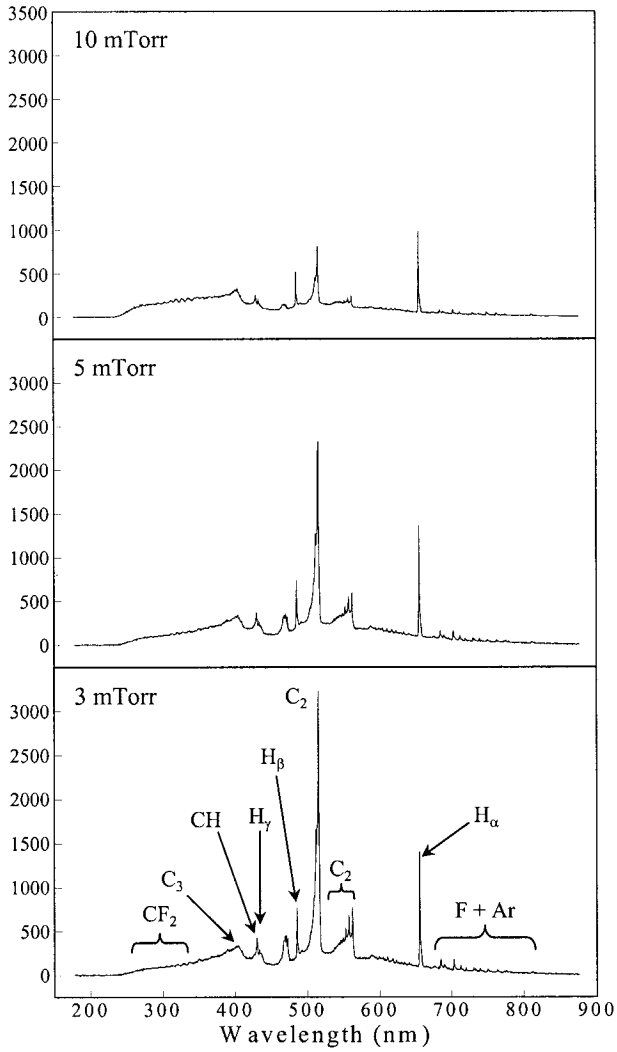

Figure 3 Optical emission spectra (OES) from 10/50 $C_2H_2F_4$ pulsed plasmas at 10, 5, and 3 mTorr, all using 50 sccm $C_2H_2F_4$. The spectra are dominated by C_2, C_3, and H species, with lower intensity CF_2 and F peaks. A small amount of Ar (2 sccm) was included as an actinometer, and each spectrum has been normalized to the 750.3 nm Ar peak intensity. There is a dramatic increase in the intensity of the C_2 peak at 516.5 nm as the pressure is reduced. At 10 mTorr the primary peak is H_α (656.2 nm), with the 516.5 nm C_2 peak is a close second. However, as the pressure is reduced, the intensity of that C_2 peak increase, strongly dominating over the H_α peak.

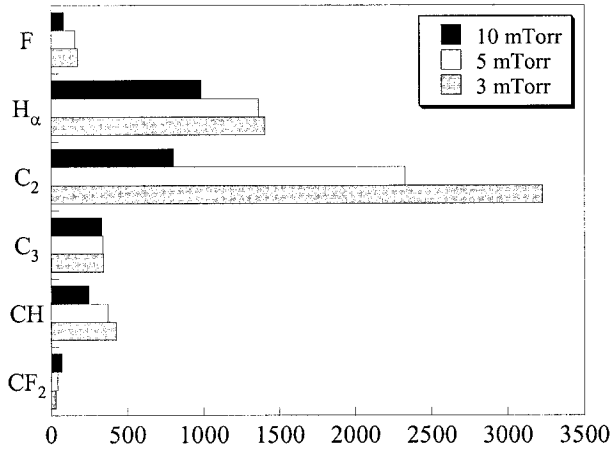

Figure 4 OES intensities of F (703.7 nm), H_α (656.2 nm), C_2 (516.5 nm), C_3 (405.1 nm), CH (431.4 nm), and CF_2 (251.9 nm) as a function of pulsed plasma pressure, all are normalized to the Ar actinometer. A large increase in intensity is seen for C_2, while more moderate increases are seen for F, H_α, and CH as pressure is reduced. Despite the changing pulsed plasma species concentrations, the deposited films are nearly identical (Fig. 2). This observation further indicates that the pulsed plasma species observed via OES may not be representative of the actual species depositing on the wafer surface.

plasma with comparatively small H_α and H_β peaks. Many of the peaks dominant in the ECR plasmas (C_2, C_3, F) are not present to any significant degree. Because an actinometer was not available for the parallel plate plasma, it is impossible to determine whether the CF_2 peaks in the ECR and parallel plate plasmas might actually represent the same concentration of CF_2. Nevertheless, one might expect the parallel plate plasma to produce more heavily fluorinated films than the ECR plasma since CF_2 is the dominant species in that plasma, as opposed to H and C_2 in the ECR plasma. However, it is actually the pulsed ECR plasma films which have the higher F : C ratios.

These observations point to key differences in the parallel plate versus ECR plasma deposition environments. The higher density of the ECR plasma will result in a higher degree of fractional ionization of the feed gas, while its higher electron temperature will lead to more efficient fracturing of molecular species in the plasma due to the larger concentration of high energy electrons.[52] These observations can account for the strong C_2, C_3, and H peaks seen in the $C_2H_2F_4$ pulsed ECR plasmas, while molecular species

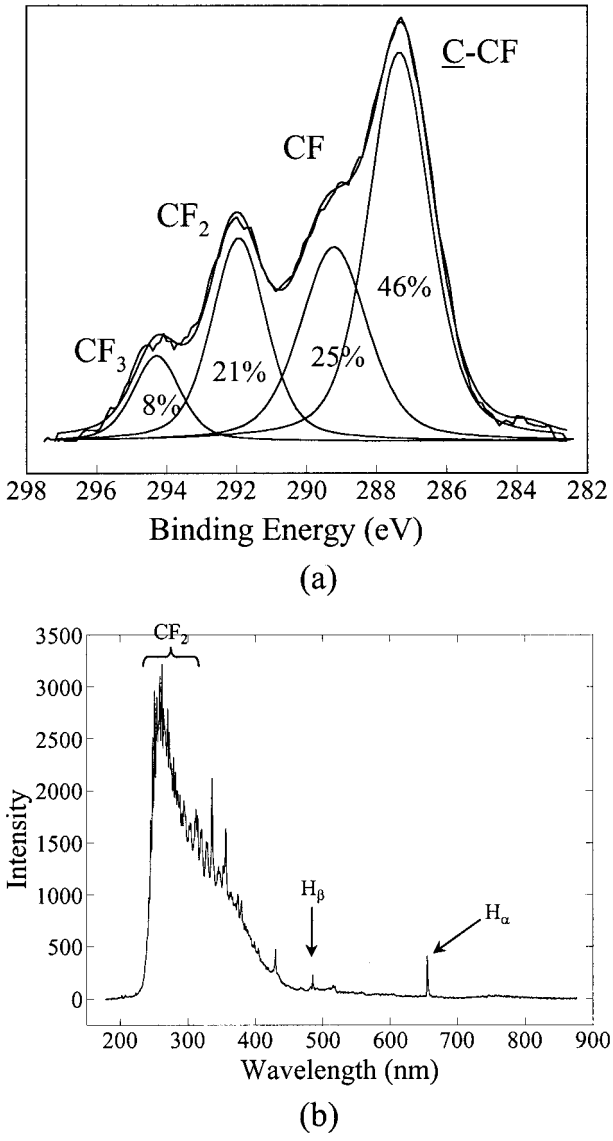

Figure 5 (a) Carbon 1s XPS spectrum for a 10/100 $C_2H_2F_4$ pulsed plasma film deposited in a parallel plate PECVD reactor. This spectrum is representative of the parallel plate pulsed plasma films from $C_2H_2F_4$, and therefore is valid for comparison to the 10/50 pulsed ECR plasma films in Figure 2. In comparison to the ECR pulsed plasma films, the parallel plate pulsed plasma film is distinctly different, most notably with a much higher C—CF fraction. (b) OES spectrum for a 10/100 $C_2H_2F_4$ parallel plate pulsed plasma. Argon actinometry was not available in the parallel plate reactor. The CF_2 OES peaks are overwhelmingly dominant in the parallel plate plasma, with comparatively small H_α and H_β peaks. Many of the peaks dominant in the ECR plasmas (C_2, C_3, F) are not present to any significant degree. The higher fluorination of the ECR plasma versus parallel plate plasma films is quite surprising given these spectra.

dominate in the pulsed parallel plate plasma. As discussed above, it is postulated that the species approaching the deposition substrate in the ECR plasma will be significantly different from those detected via the OES fiber located ~ 8 in. above the substrate.[46–49] Gas-phase recombinations are expected to occur between the OES fiber and the substrate, and thus CF_x (x = 1–3) deposition species, as well as F addition to a carbonaceous surface, can contribute to the formation of a highly fluorinated film. The parallel plate plasma does not reduce the feed gas to its constituent components as readily as the ECR plasma, so many of the recombination reactions present in the ECR system are not available. The other major difference between the ECR and parallel plate systems is the presence of ion bombardment in the parallel plate reactor. No wafer biasing is used in the ECR depositions, so ion bombardment is negligible. Ion bombardment has been shown to defluorinate films; therefore, the lower fluorination of the parallel plate films can be partially attributed to this effect.[53]

CONCLUSIONS

Pulsed ECR plasmas from 1,1,2,2-$C_2H_2F_4$ have been used to deposit fluorocarbon films. The deposited films have a F : C ratio of 1, with only slight variations in % CF_x as deposition pressure is decreased. OES spectra of the pulsed $C_2H_2F_4$ plasmas show high intensity peaks for H, C_2, and C_3, with lower intensity CF_2 and F peaks. The dominant OES peak shifts from H_α to C_2 when the pressure is reduced, most likely a result of the increased electron temperature at the lower pressure. Gas-phase recombination reactions may be occurring between the OES sampling region and the deposition substrate, producing fluorocarbon molecular deposition species, and thus accounting for the high degree of fluorination in the deposited films. Parallel plate plasma deposited films from $C_2H_2F_4$ show less fluorination than their ECR counterparts, as well as vastly different OES spectra, with CF_2 peaks dominating the spectra versus H and C_2. The presence of ion bombardment in the parallel plate system tends to defluorinate depositing films and thus can account for the less fluorinated films deposited in the parallel plate versus ECR systems.

The authors gratefully acknowledge the use of MRSEC Shared Facilities.

REFERENCES

1. Wolf, S. Silicon Processing for the VLSI Era; Lattice Press: Sunset Beach, CA, 1990; Vol. 2.
2. Sze, S. M. VLSI Technology; McGraw–Hill: New York, 1983.
3. Yasuda, H. Plasma Polymerization; Academic: New York, 1985.
4. d'Agostino, R., Ed. Plasma Deposition, Treatment, and Etching of Polymers; Academic: Boston, 1990.
5. Cote, D. R.; Nguyen, S. V.; Stamper, A. K.; Armbrust, D. S.; Tobben, D.; Conti, R. A.; Lee, G. Y. IBM J Res Dev 1999, 43, 5.
6. Singer, P. Semicond Int 1994, 17(13), 52.
7. Laxman, R. K. Semicond Int 1995, 18(5), 71.
8. Singer, P. Semicond Int 1996, 19(5), 88.
9. Peters, L. Semicond Int 1998, 21(10), 64.
10. Endo, K. MRS Bull 1997, 22(10), 55.
11. Savage, C. R.; Timmons, R. B.; Lin, J. W. In Structure–Property Relations in Polymers: Spectroscopy and Performance; Urban, M. W.; Craver, C. D., Eds.; American Chemical Society: Washington, DC, 1993; Vol. 236, p 745.
12. Gleason, K. K. In History and Future of Fluorocarbon CVD Low Kappa Dielectric Thin Films; VMIC: Santa Clara, CA, 1999; p 11.
13. Endo, K.; Tatsumi, T. Appl Phys Lett 1996, 68, 2864.
14. Takahashi, K.; Hori, M.; Kishimoto, S.; Goto, T. Jpn J Appl Phys Part 1 1994, 33(7B), 4181.
15. Oehrlein, G. S.; Zhang, Y.; Vender, D.; Haverlag, M. J Vac Sci Technol A 1994, 12, 323.
16. Wang, J.-H.; Chen, J.-J.; Timmons, R. B. Chem Mater 1996, 8, 2212.
17. Takahashi, K.; Hori, M.; Goto, T. J Vac Sci Technol A 1996, 14, 2011.
18. Takahashi, K.; Hori, M.; Goto, T. J Vac Sci Technol A 1996, 14, 2004.
19. Ma, Y.; Yang, H.; Guo, J.; Sathe, C.; Agui, A.; Nordgren, J. Appl Phys Lett 1998, 72, 3353.
20. Takeishi, S.; Kudo, H.; Shinohara, R.; Hoshino, M.; Fukuyama, S.; Yamaguchi, J.; Yamada, M. J Electrochem Soc 1997, 144, 1797.
21. Mountsier, T. W.; Samuels, J. A. Thin Solid Films 1998, 332, 362.
22. Endo, K.; Tatsumi, T. Appl Phys Lett 1997, 70, 2616.
23. Limb, S. J.; Edell, D. J.; Gleason, E. F.; Gleason, K. K. J Appl Polym Sci 1998, 67, 1489.
24. Haverlag, M.; Stoffels, W. W.; Stoffels, E.; Kroesen, G. M. W.; de Hoog, F. J. J Vac Sci Technol A 1996, 14, 384.
25. Labelle, C. B.; Gleason, K. K. J Vac Sci Technol A 1999, 17, 445.
26. Labelle, C. B.; Karecki, S.; Reif, R.; Gleason, K. K. J Vac Sci Technol A 1999, 17, 3419.
27. Savage, C. R.; Timmons, R. B.; Lin, J. W. Chem Mater 1991, 3, 575.

28. Limb, S. J.; Gleason, K. K.; Edell, D. J.; Gleason, E. F. J Vac Sci Technol A 1997, 15, 1814.
29. Fujiwara, N.; Maruyama, T.; Miyatake, H. Jpn J Appl Phys Part 1 1998, 37(4B), 2302.
30. Samukawa, S. Jpn J Appl Phys Part 1 1993, 32(12B), 6080.
31. Samukawa, S. Appl Phys Lett 1994, 64, 3398.
32. Ahn, T. H.; Nakamura, K.; Sugai, H. Plasma Sources Sci Technol 1996, 5, 139.
33. Hynes, A. M.; Shenton, M. J.; Badyal, J. P. S. Macromolecules 1996, 29, 4220.
34. Hynes, A.; Badyal, J. P. S. Chem Mater 1998, 10, 2177.
35. Takahashi, K.; Hori, M.; Goto, T. Jpn J Appl Phys Part 2 1993, 32(8A), L1088.
36. Takahashi, K.; Hori, M.; Maruyama, K.; Kishimoto, S.; Goto, T. Jpn J Appl Phys Part 2 1993, 32(5A), L694.
37. Takahashi, K.; Hori, M.; Goto, T. Jpn J Appl Phys Part 1 1994, 33, 4745.
38. Coburn, J. W.; Chen, M. J Appl Phys 1980, 51, 3134.
39. Kiss, L. D. B.; Nicolai, J.-P.; Conner, W. T.; Sawin, H. H. J Appl Phys 1992, 71, 3186.
40. Gottscho, R. A.; Donnelly, V. M. J Appl Phys 1984, 56, 245.
41. d'Agostino, R.; Colaprico, V.; Cramarossa, F. Plasma Chem Plasma Process 1981, 1, 365.
42. d'Agostino, R.; Cramarossa, F.; De Benedictis, S.; Ferraro, G. J Appl Phys 1981, 52, 1259.
43. Reader, J.; Corliss, C. H. Wavelengths and Transition Probabilities for Atoms and Atomic Ions; National Bureau of Standards: Washington, DC, 1980; Vol. 1.
44. Pearse, R. W. B.; Gaydon, A. G. The Identification of Molecular Spectra, 3rd ed.; Chapman & Hall; London, 1963.
45. Atkins, P. W. Physical Chemistry, 4th ed.; W. H. Freeman & Company: New York, 1990.
46. Farhat, S.; Findeling, C.; Silva, F.; Hassouni, K.; Gicquel, A. J Phys IV 1998, 8(P7), 391.
47. Mitsuda, Y.; Kojima, Y.; Yoshida, T.; Akashi, K. J Mater Sci 1987, 22, 1557.
48. Saito, Y.; Matsuda, S.; Nogita, S. J Mater Sci Lett 1986, 5, 565.
49. Saito, Y.; Sato, K.; Tanaka, H.; Fujita, K.; Matuda, S. J Mater Sci 1988, 23, 842.
50. Forster, J.; Holber, W. J Vac Sci Technol A 1989, 7, 899.
51. Angra, S. K.; Kumar, P.; Banerfie, P. C.; Bajpai, R. P. Thin Solid Films 1997, 304, 294.
52. Graves, D. B. IEEE Trans Plasma Sci 1994, 22, 31.
53. O'Keefe, M. J.; Rigsbee, J. M. J Appl Polym Sci 1994, 53, 1631.